



WEAR AND SURFACE ROUGHNESS OF 3D PRINTED AND MILLED CAD-CAM RESTORATIVE MATERIALS

Ahmed Mohamed Arafa^{1*}, Lomaya Ghanem²

ABSTRACT

Objective: to assess wear behavior and surface roughness of CAD-CAM restorative materials and their opposing enamel antagonists. **Materials and methods:** Rectangular-shaped specimens (n=22) (14×12×1.5 mm) were prepared; 3D printed VarseoSmile Crown plus (VS) (n=11) and milled brilliant crios (BC) (n=11). Both groups were finished with composite polishing kit. Wear testing was performed in chewing simulator with twenty-two freshly extracted mandibular premolars antagonists. The wear of specimens and opposing enamel antagonists was calculated by weight loss. The surface roughness (Ra) of the specimens and their opposing enamel antagonist was analyzed by using a digital image analysis software at baseline and after chewing simulation then inspected by SEM. Data were statistically analyzed using Paired t-test, Independent t-test, and Chi square test ($p = 0.05$). **Results:** A significant weight loss in tested groups and their opposing enamel antagonists after chewing simulation was noticed by Paired t-test ($p < 0.05$) where insignificant percentage change of weight between tested groups ($p = 0.93$) and between their antagonists ($p = 0.79$) was noticed by Chi square test. Also, A significant difference in Ra value after chewing simulation between tested groups was noticed ($p < 0.05$) where insignificant percentage change in Ra value between tested groups ($p = 0.74$) and between their antagonists ($p = 0.88$) was noticed by Chi square test. **Conclusions:** Based on their properties, each material was affected by chewing simulation at different intensities; The tested CAD-CAM restorative materials and their opposing enamel antagonists showed wear demonstrated by weight loss and difference in surface roughness.

KEYWORDS: Wear, Surface roughness, 3D printing, CAD-CAM, Resin-matrix ceramics

INTRODUCTION

Indirect restoration fabrication using CAD-CAM systems in fixed prosthodontics has undergone several innovations over the last decade. This results in widespread use for both laboratory and in-office ones due to their simplicity, decreasing the human variations with reduced time and cost. Therefore, more reliable made, precise prostheses can be obtained from a uniform design and fabrication process by skillful technicians with fewer errors than the conventional method, specifically steps such as impression-making, waxing, and casting⁽¹⁾.

In dentistry, subtractive manufacturing using CNC machines resulted in a prosthesis with fewer porosities and a more homogenous consistency from solid materials (blocks and discs)⁽¹⁾. Additive manufacturing is an alternative method that includes 3D printing technologies in which the creation of a 3D object⁽²⁾ through the fusion of liquid or powder materials together layer by layer. It is commonly used to produce metal copings, provisional restorations, occlusal splints, surgical guides, and removable prostheses⁽¹⁾. Compared to subtractive manufacturing, additive manufacturing has many

1. Lecturer of Fixed Prosthodontics, Faculty of Dentistry, Beni-Suef University, Beni-Suef, Egypt.

2. Associate Professor of Fixed Prosthodontics, Faculty of Oral and Dental Medicine, Misr International University, Cairo, Egypt.

• **Corresponding author:** ahm.arafa@dent.bsu.edu.eg

advantages due to less material waste, the ability to produce larger objects, and fine detail production^(1,3).

Several years of innovation in 3D printing technology allow the printing of the digital object from a polymeric material in layers that are deposited in the XY plane as a cross-sectional slice on a movable platform in the Z-axis degree. It includes digital light processing (DLP), stereolithography (SLA), material jetting (MJ), fused deposition modeling (FDM), and selective laser doping (SLS)⁽³⁾.

The more common in-office 3D printers are SLA and DLP types which are similar in the use of a monomeric resin, producing prosthetics through photo-polymerization⁽⁴⁾. They differ in that DLP utilizes a light projector to polymerize a full resin layer in the XY-axis simultaneously, while in SLA, a moving laser beam is the light source⁽³⁾ that sweeps across the resin tank to solidify the material layer by layer on the horizontal axis. Although the DLP method is a promising technology in dentistry due to its rapid processing with high resolution and low cost⁽³⁾, it does not offer the same homogenous surface finish and texture in the printed object as SLA because of the pixel projection. In SLA, the point-by-point resin polymerization on the print bed leads to no loss of surface quality making this technology ideal for millimeter-scale printing⁽⁴⁾.

Nowadays with the continuous evolution of light-cured resin composite materials, the 3D printing of adhesively cemented restorations becomes possible as a treatment option⁽⁵⁾. VarseoSmile Crown plus (VS) is a newly developed tooth-colored, ceramic-filled hybrid resin material, light-cured plastic based on methacrylic acid esters. Their ability to withstand high occlusal forces allows the manufacturing of inlays, onlays, veneers, and permanent crowns⁽⁵⁾. On the side, different families of materials are available for subtractive manufacturing of desired restorations through CAD-CAM technology with acceptable mechanical, physical, and esthetic properties⁽⁶⁾. It includes glass-matrix ceramics, polycrystalline ceramics, and resin-matrix ceramics⁽⁷⁾.

The exclusively introduced resin-matrix ceramics for CAD-CAM combine advantages of both organic and inorganic phases of parent ceramics and resins. It offers shock-absorbing ability due to its modulus of elasticity that is very close to those of dentin, and friendly to opposing enamel antagonists. The improved fracture resistance makes it advisable in the area with high occlusal loads⁽⁸⁾. Moreover, easy milling and polishing procedures in addition to simplified intra-oral repair with composite resin add more benefits for their clinical use in single-visit restoration^(7,9). This improvement in the mechanical properties of CAD-CAM composites (flexural strength ~ 200–300 MPa) was attributed to polymerization under high pressure and temperature⁽¹⁰⁾.

Brilliant Crios (BC) (Coltène, Whaledent A.G. Altstätten, Switzerland) is one of the available materials for subtractive manufacturing which is reinforced composite resin with amorphous silica and glass ceramic fillers in a cross-linked methacrylate matrix having a modulus of elasticity 10.3 GPa⁽¹¹⁾.

Wear resistance is an important physical property in dentistry as it can predict the durability and longevity of different restorative materials during function⁽¹¹⁾. Excessive wear may reduce the vertical dimension of occlusion causing premature contact in the anterior segment, reduction in the masticatory efficiency, muscles of mastication fatigue, and impaired esthetics⁽¹¹⁾. In parallel, the surface roughness of restorative materials is another crucial factor affecting plaque accumulation, staining ability, shade and resultant patient satisfaction⁽¹²⁾. In addition, the surface finish of the restoration and antagonist plays a significant role in wear.

Although the complexity of both the masticatory system and the wear process, wear simulation research can predict wear rates of different materials and opposing enamel antagonists to compare these results with a standard material of proved acceptable laboratory and clinical performance⁽¹³⁾.

Lack of available data on the wear behavior and surface roughness of newly introduced 3D printed, and their opposing enamel antagonists is critical to have proper selection criteria for the restorative material.

So, this study aimed to assess the wear behavior and surface roughness of CAD-CAM restorative materials whether 3D printed or milled, and their opposing enamel antagonist. The tested null hypotheses of this study were that no difference would be found: (1) in the wear behavior of the tested 3D printed or milled CAD-CAM restorative materials under increased loads, (2) in the wear behavior of the opposing enamel antagonists, (3) in the surface roughness of the tested 3D printed or milled CAD-CAM restorative materials at baseline and after chewing simulation, (4) in the surface roughness of the opposing enamel antagonists

at baseline and after chewing simulation and that (5) there will be no correlation between the wear behavior and the surface roughness of both the tested 3D printed and milled CAD-CAM restorative materials and their opposing enamel antagonists.

MATERIALS AND METHODS

Sample size was detected according to a previous study ⁽¹⁴⁾ in which 9 per group was the minimally accepted sample size when the response within each subject group was normally distributed with a standard deviation of 0.49, the true mean difference was 0.68 when the power was 80 % & type I error probability was 0.05. Sample size increased to 11 per group to compensate 15 % dropout. The details of the materials' composition and their filler content utilized in this study are listed in Table 1.

TABLE (1) Materials' composition and their manufacturers utilized in the study.

Trade name	Manufacturer	Composition	Filler Mass (weight %)	Modulus of elasticity
Varseo Smile	Bego, Bremen, Germany	- 40-isopropyl lidiphenol, ethoxylated and 2-methylprop-2enoic acid.	0.7 μ m particle size forming	4.09 GPa
Crown plus (VS)		- Silanized dental glass, methyl benzoyl formate, diphenyl (2,4,6-trimethyl benzoyl) phosphine oxide.	30–50 wt. % inorganic filler	
Brilliant Crios (BC)	Coltène, Whaledent A.G. Altstätten, Switzerland	- 70.7% <20 nm Amorphous silica and <1 μ m barium glass. - 29.3% Cross-linked methacrylate resin matrix (Bis-GMA, Bis-EMA, TEGDMA)	(SiO ₂ < 20 nm, barium glass <1 μ m forming 70.7 wt.% inorganic filler	10.3 GPa

Bis-GMA, bisphenol A-glycidyl methacrylate, Bis-EMA, ethoxylated bisphenol A-glycol dimethacrylate, TEGDMA, triethylene glycol dimethacrylate; UDMA urethane dimethacrylate, SiO₂, silicon dioxide.

Teeth specimen preparation:

Twenty-two recently extracted mandibular first premolars for orthodontic causes were selected having intact crowns without abrasion cavities and/or caries. (All procedures were performed after the approval of the Research Ethics Committee (FDBSU-REC) of Faculty of Dentistry, Beni-Suef University, Egypt (Approval number: # REC-FDBSU/03112022-03/AA).

The selected teeth were stored in 0.9% saline (ADWIC, Pharmaceutical division, Abu Zabal, Egypt) after scaling to remove any organic debris until testing procedures to prevent dehydration during storing time. In order to standardize the acrylic blocks, a machine-milled split brass mold was used to vertically mount the tooth specimen in self-curing poly-methyl-methacrylate (PMMA) resin (Acrostone, Egypt), along its long axis. Teeth specimens were centralized in the mold at a predetermined depth using a paralleling device (BEGO, Germany) until resin blocks polymerize completely then stored again in 0.9% saline.

3D printed discs fabrication:

STL file of rectangular-shaped discs with desired dimensions (14×12×1.5 mm) was designed using a

software program (exocad Dental DB 3.0 Galway, exocad GmbH, USA). The finished STL file was printed using DLP technology utilizing a 3D printer (Anycubic photon S, Shenzhen, China). The composite resin discs were printed vertically to the platform from a liquid material VarseoSmile plus (VS) as shown in Figure 1. 3D printing preprocessing software (Chitubox V1.9.0, Shenzhen, China) was used to prepare resin optimized for VS with a layer height 0.05 mm, bottom layer count 8, exposure time 6.5s, bottom exposure 20s, lift distance 5 mm and lift speed 60 mm/s.

On completion of printing, the eleven 3D printed specimens were separated from the build platform using the spatula and then were cleaned following manufacturing recommendation in two steps with ethanol (96 %) using an unheated ultrasonic bath (Anycubic 3D Printer Wash and Cure Machine 2.0). First, for 3 min in a reusable ethanol solution (96 %) then cleaned carefully for another 2 min in a freshly used ethanol (96 %) solution. Finally, the 3D printed specimens were removed from the ethanol bath and sprayed with additional ethanol (96 %) to totally get rid of any remaining resin residue. After cleaning, the 3D printed specimens were dried using compressed air under an extraction unit.

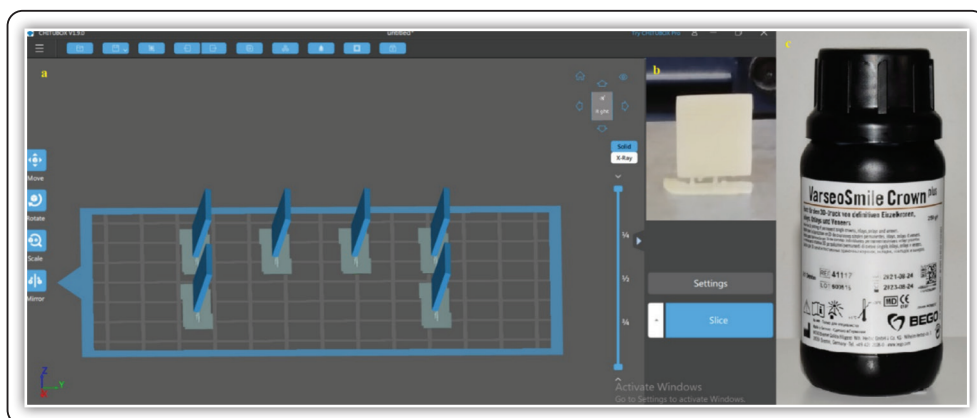


FIG (1) 3D printed (VS) specimens using a 3D printer (a) pre-processing before 3D printing. (b) printed specimen on build platform of the 3D printer. (c) Varseo Smile Crown plus composite resin bottle.

The post-curing of the printed specimens was performed two times for 45 min, then left to cool for 3-5 min in an ultraviolet light curing device (Anycubic 3D Printer Wash and Cure Machine 2.0) suitable for post-curing of 3D printed composite resin materials to ensure full polymer conversion reducing residual monomer thus obtaining the highest mechanical properties. Cutting of all supporting structures of the final printed end product was performed with cutting wheel.

Milled discs fabrication:

Eleven rectangular-shaped discs with desired dimensions (14×12×1.5 mm) were cut of Brilliant Crios (BC) CAD-CAM blocks (Coltène, Whaledent A.G. Altstätten, Switzerland) using an electrical high-precision saw (Isomet 4000, micro-saw, Buehler Ltd, USA) under water cooling system with two anticorrosive agents rotating at a speed 2500 rpm and feeding rate 5 mm/min utilizing diamond disc (Buehler instrument, USA) with a thickness of 0.6 mm.

Finishing of discs:

After checking the final thickness for all specimens of tested groups using a digital caliper to have a thickness of 1.5 mm with an accuracy of ± 0.01 mm, all specimens of tested CAD-CAM restorative materials (n=22) were secured in a teflon mold using self-curing poly-methyl-methacrylate (PMMA) resin blocks (Acrostone, Egypt) to match the jig of chewing simulator then finished with a composite polishing kit (AZDENT RA0309, Mainland, China) according to a previous study⁽¹⁵⁾ to get a perfect smooth surface. All specimens of tested groups and enamel antagonists were steam cleaned, dried with absorbent paper then air dried before weighing.

Wear testing procedures:

Two-body wear testing was performed under a load of 98 N for 60000 cycles simulating 6 months of clinical use⁽¹⁶⁾ in a chewing simulator (Robota,

model ACH-09075DC-T, AD Tech technology Co. Ltd, Frankfurt, Germany) having four chambers resembling the horizontal and vertical movements simultaneously with thermocycling to perform two-body wear in distilled water. Each chamber consists of an upper Jakob's chuck as an antagonist holder that can be tightened with a screw and a lower plastic specimen holder to which the tested specimen can be attached. A schematic diagram representing the wear testing configuration is presented in Figure 2 and the wear testing parameters are presented in Table 2.

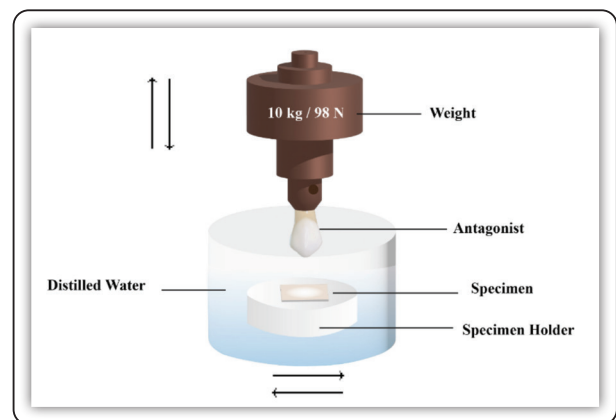


FIG (2) Schematic diagram of chewing simulation.

TABLE (2) Wear testing parameter applied in the study.

Wear testing parameters	
Cold/hot bath temperature: 5°C/55°C	Horizontal movement: 3mm
Vertical movement: 3 mm	Forward speed: 40 mm/s
Rising speed: 90 mm/s	Backward speed: 40 mm/s
Descending speed: 40 mm/s	Weight per specimen: from 10 kg
Cycle frequency 1.6 Hz	Torque; 2.4 N.m
Dwell time: 60 s	

After completion of wear testing procedures, all tested specimens and their opposing enamel antagonists were retrieved, dried with paper towels,

and compressed air then weighed again. Wear quantification of specimens and their opposing enamel antagonists was calculated by weight loss using an analytical balance (Quintix124-1S, Sartorius AG, Göttingen, Germany) with 0.0001 gm accuracy to determine the variation in weight at baseline and after 60000 cycles of chewing simulation.

Scanning electron microscope (SEM) (Quanta FEG 250, FEI Company, Hillsboro, Oregon-USA) was used to examine a representative specimen from each tested group at baseline and after the wear testing procedures at 10.1 mm distance with an excitation voltage of 20 kV at different magnification.

A digital image analysis software (WSxM, Ver 5 develop 4.1, Nanotec, Electronica, SL, San Diego, CA) coupled with a USB Digital microscope having a built-in camera (U500X Capture Digital Microscope, Guangdong, China) fixed at a magnification of 120X connected to a personal computer was utilized to build up a 3D image of the specimens' surface profile and their antagonist enamel at baseline and after wear testing procedures. The images were saved with a resolution of 1280 × 1024 pixels per image then cropped to 350 x 400 pixels to identify the selected area measuring roughness⁽¹⁷⁾ then analysis was performed by using software to turn the pixels into absolute units by comparing a ruler with a scale of software to determine the average of heights (Ra) expressed in microns (μm) which is a reliable index of surface roughness⁽¹⁸⁾.

Data were presented as mean and standard deviation for values. Shapiro-Wilk test and Kolmogorov-Smirnov test were used to explore the given data for normality. It revealed that both tested groups regarding specimens and their opposing enamel antagonists originated from normal distribution (parametric data) resembling normal Bell curve. Accordingly, a comparison between different intervals was performed by using Paired t-test, a comparison between different groups was performed by Independent t-test and Chi square test was used to compare between percentage changes.

Significance was set at $p \leq 0.05$. Statistical analysis was performed with a statistical software program (IBM SPSS 16[®] Statistical Package for Scientific Studies, IBM Corp).

RESULTS

Regarding the wear behavior, the mean values, standard deviations, and statistical results of the weight loss recorded in gm for the tested groups and their opposing enamel antagonists at baseline and after 60000 cycles of chewing simulation were listed in Table 3.

Paired t-test revealed a significant weight loss (wear) in all tested CAD-CAM restorative materials and in their opposing enamel antagonists after chewing simulation ($p < 0.05$). Chi square test revealed an insignificant percentage change of weight between tested groups ($p = 0.93$) and between their opposing enamel antagonists ($p = 0.79$) where a higher percentage change of weight was found in VS group (-1.09%) and their opposing enamel antagonists (-1.32%).

Regarding the surface roughness evaluation, the mean values, standard deviations, and statistical results recorded in μm for the tested groups and their opposing enamel antagonists at baseline and after 60000 cycles of chewing simulation were listed in Table 4.

Paired t-test revealed an insignificant difference in Ra value of the 3D printed (VS) group and their opposing enamel antagonists ($p > 0.05$). A significant reduction in Ra value was found in the milled (BC) group ($p < 0.05$), while their opposing enamel antagonists showed insignificant differences ($p > 0.05$). Chi square test revealed an insignificant percentage change in Ra value between tested groups ($p = 0.74$) and between their opposing enamel antagonists ($p = 0.88$) where a higher percentage change of Ra was found in milled (BC) group (-3.57%) their opposing enamel antagonists (-0.53%).

TABLE (3) Mean and standard deviation of 3D printed and milled groups regarding specimens and antagonists' weight (gm) at baseline and after chewing simulation and comparison between them:

Weight		3D Printed group (VS)		Milled group (BC)		Difference			
						MD ± SEM	P value	95% CI	
		M	SD	M	SD			L	U
Specimen	Baseline	0.3651	0.0038	0.5175	0.0214	-0.152 ± 0.006	<0.0001*	-0.16	-0.13
	After	0.3616	0.0029	0.5135	0.0201	-0.152 ± 0.006	<0.0001*	-0.16	-0.12
	P value	0.0001*		0.004*					
	Change%	-1.09		-0.77			0.93		
Antagonist	Baseline	1.0587	0.1565	0.9031	0.1083	0.155 ± 0.05	0.009*	0.04	0.26
	After	1.0442	0.1482	0.9003	0.1088	0.144 ± 0.05	0.01*	0.03	0.25
	P value	0.001*		0.0001*					
	Change%	-1.32		-0.29			0.79		

M: mean, SD: standard deviation, Change %: percentage of change, MD: mean difference, SEM: standard error of mean, CI: confidence interval. *Significant difference as p <0.05

TABLE (4) Mean and standard deviation of 3D printed and milled groups regarding specimens and antagonists surface roughness (µm) at baseline and after chewing simulation and comparison between them:

Surface roughness (Ra)		3D Printed group (VS)		Milled group (BC)		Difference			
						MD ± SEM	P value	95% CI	
		M	SD	M	SD			L	U
Specimen	Baseline	0.2596	0.0045	0.2605	0.0041	-0.0009 ± 0.002	0.61	-0.004	0.001
	After	0.2562	0.0036	0.2512	0.0007	0.005 ± 0.001	0.0001*	0.002	0.007
	P value	0.052		0.0001*					
	Change %	-1.31		-3.57			0.74		
Antagonist	Baseline	0.2604	0.0029	0.2613	0.0045	-0.0009 ± 0.002	0.56	-0.004	0.002
	After	0.26	0.0019	0.2599	0.0062	0.01 ± 0.002	0.59	-0.003	0.004
	P value	0.65		0.53					
	Change %	-0.15		-0.53			0.88		

M: mean, SD: standard deviation, Change %: percentage of change, MD: mean difference, SEM: standard error of mean, CI: confidence interval. *Significant difference as p <0.05

There was insignificant weak correlation between surface roughness and weight loss of both tested groups and their opposing enamel antagonists

calculated by using Pearson's correlation coefficient as listed in Table 5.

TABLE (5) Correlation between surface roughness (Ra) and weight loss of both groups:

			r	P	Indication
3D Printed group (VS)	Specimen	Ra Weight	0.15	0.47	Insignificant / Weak / Positive
	Antagonist	Ra Weight	0.01	0.9	Insignificant / Weak / Positive
Milled group (BC)	Specimen	Ra Weight	0.27	0.19	Insignificant / Weak / Positive
	Antagonist	Ra Weight	0.22	0.29	Insignificant / Weak / Positive

Representative SEM images of the tested groups are presented in Figure 2 and 3. All tested specimens showed wear scar with few detached fillers with

sliding direction of enamel antagonists on the worn surface indicating an abrasive wear behavior.

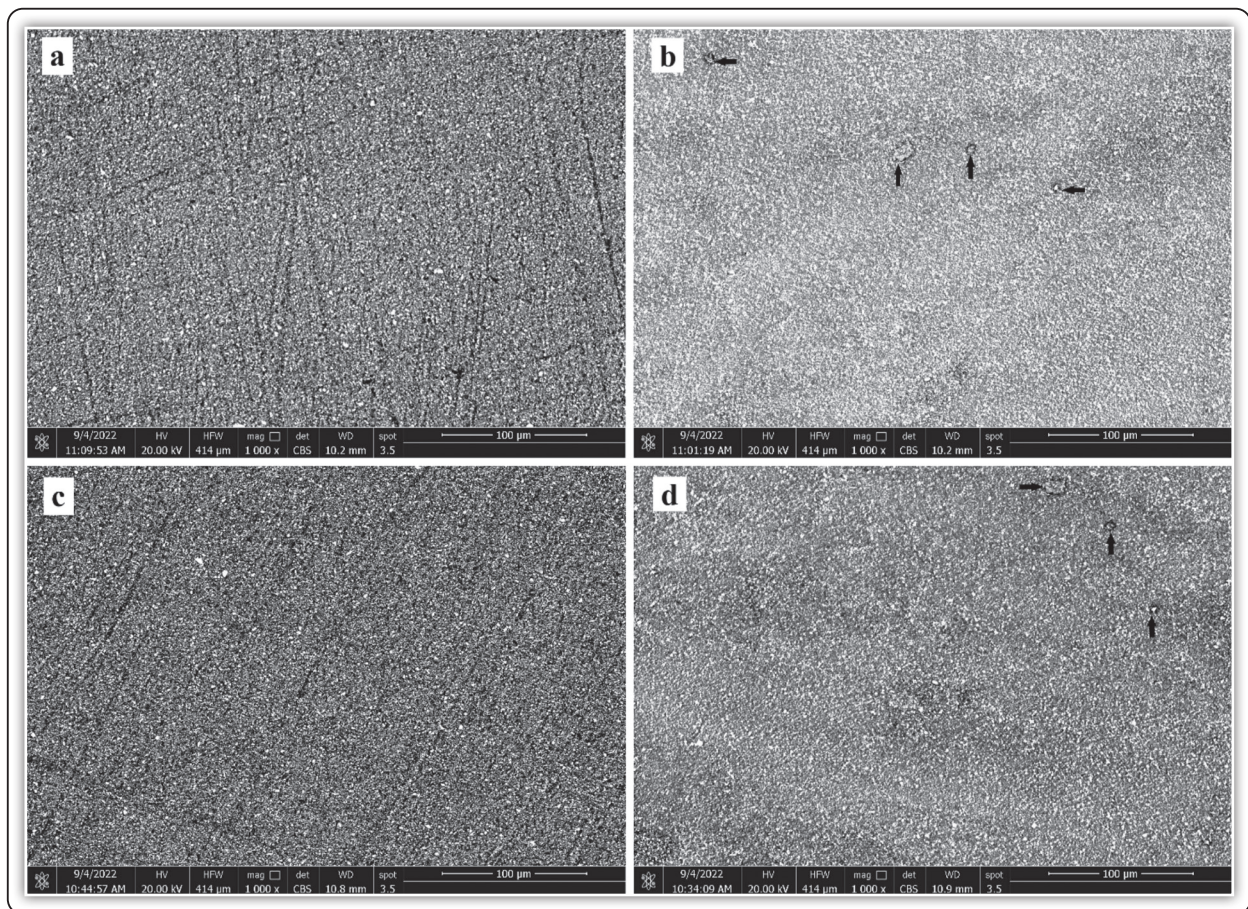


FIG (3) SEM of tested CAD-CAM restorative materials (1000x): (a) VS specimen at baseline showing very shallow and superficial flaws, grooves. (b) VS after chewing simulation, arrows showing very few detached fillers. (c), BC specimen at baseline showing very shallow and superficial flaws, grooves. (d), BC specimen after chewing simulation, arrows showing very few detached fillers.

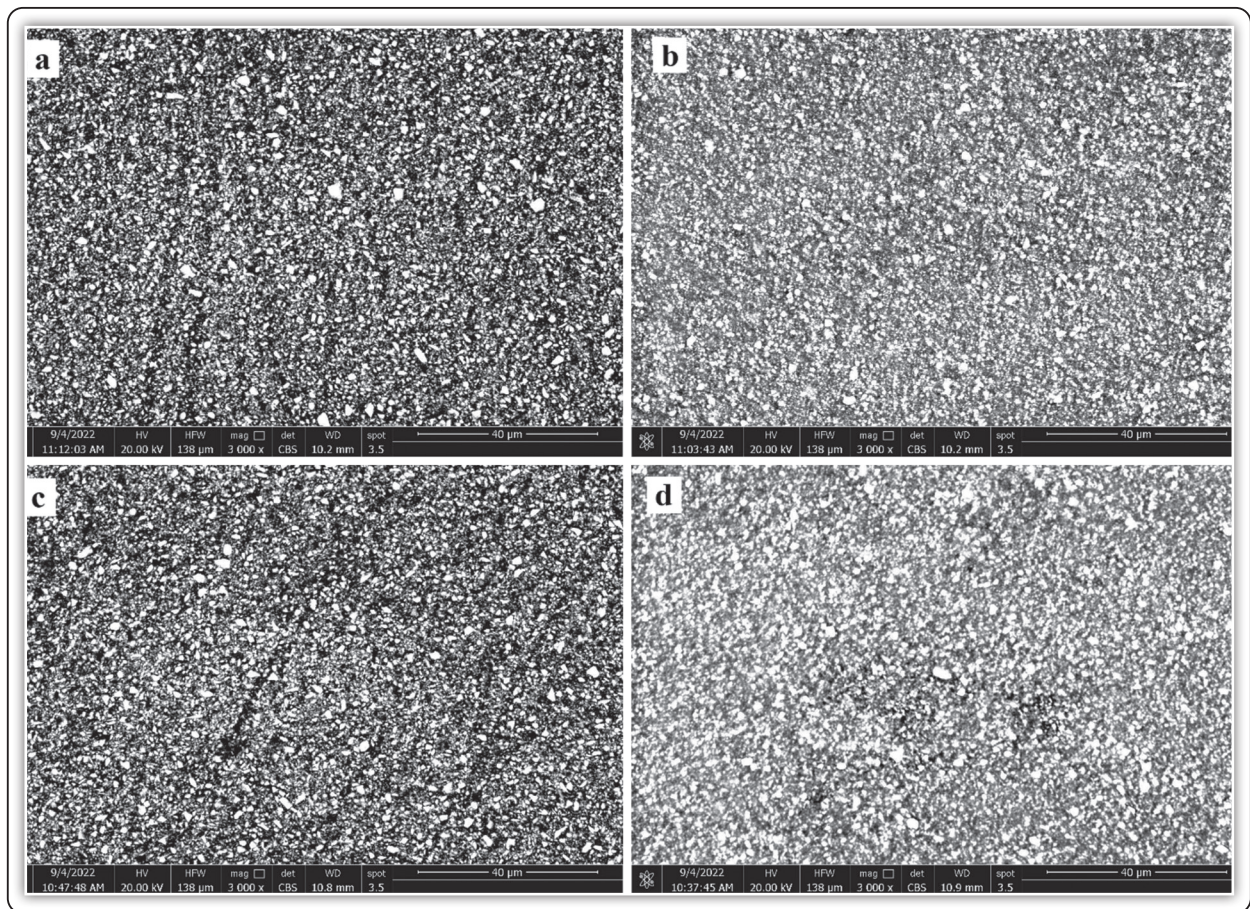
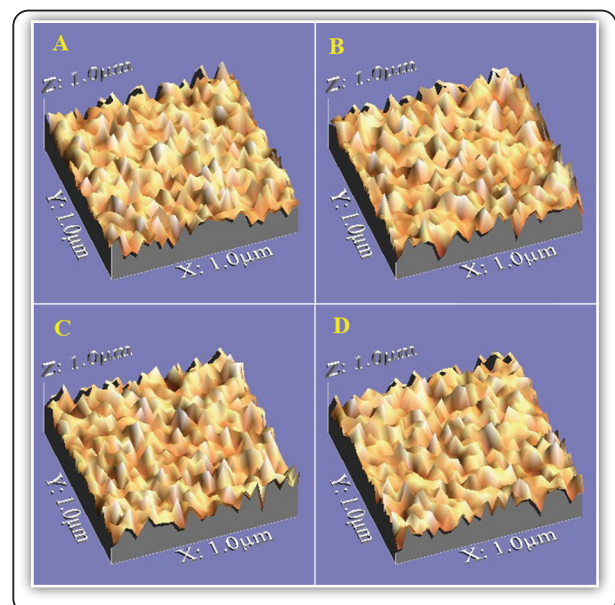


FIG (4) SEM of tested CAD-CAM restorative materials (3000x) showing similar filler distribution (a) VS specimen at baseline. (b) VS specimen after chewing simulation. (c) BC specimen at baseline. (d) BC specimen after chewing simulation.

Representative 3D images of the surface profile of tested groups and their opposing antagonist enamel at baseline and after wear chewing simulation are presented in Figures 4 and 5. The 3D images revealed an insignificant reduction of Ra for the tested groups and their opposing antagonist enamel after chewing simulation except for the milled group (BC) with a pattern of lower peaks and shallower valleys.

FIG (5) Representative 3D images of the surface profile of tested groups A: VS specimen at baseline, B: VS specimen after chewing simulation, C: BC specimen at baseline, and D: after chewing simulation.



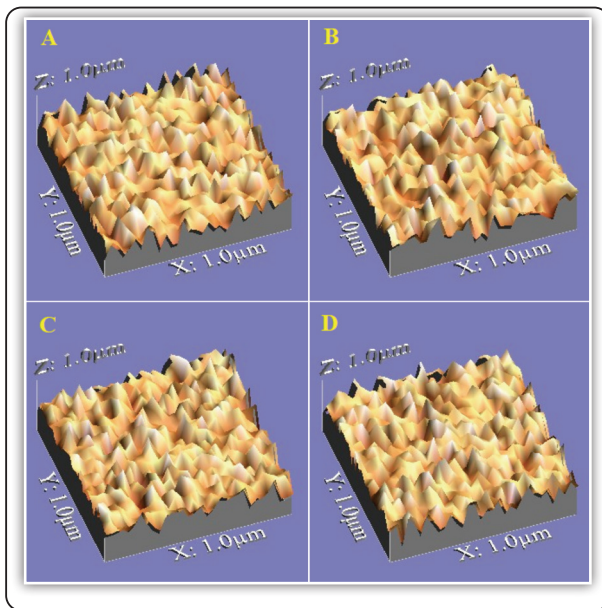


FIG (6) Representative 3D images of the surface profile of antagonist enamel. A: antagonist enamel at baseline to VS specimen, B: antagonist enamel after chewing simulation to VS specimen. C, antagonist enamel at baseline to BC specimen. D: antagonist enamel after chewing simulation to BC specimen.

DISCUSSION

In this in-vitro study, assessment of the wear behavior and surface roughness of CAD-CAM restorative materials whether 3D printed (VS) or milled (BC), and their opposing enamel antagonist was performed. The first and second null hypotheses of the study was rejected. The results of the study showed a significant reduction in weight (weight loss) in the 3D printed (VS), milled (BC) and their opposing enamel antagonists after chewing simulation ($p < 0.05$). Nevertheless an insignificant percentage change of weight was noticed between tested groups ($p = 0.93$) and between their opposing enamel antagonists ($p = 0.79$), a higher percentage change of weight was found in VS group (-1.09%) and their opposing enamel antagonists (-1.32%).

This may be attributed to relatively low filler content (about 30-50 wt. % inorganic fillers with 0.7 μm particle size)⁽¹⁹⁾ with low modulus of elasticity (4.09 GPa) compared to hard dental tissue in

addition to damage caused by mechanical abrasion and chemical degradation induced by hydrolysis effect of water⁽²⁰⁾. On the other side, the milled group (BC) and their opposing enamel antagonists revealed the least percentage change of weight which may be attributed to higher filler content (about 70.7 wt.% inorganic filler with a mixture of small-sized ($\text{SiO}_2 < 20 \text{ nm}$) and medium-sized fillers (barium glass $< 1 \mu\text{m}$) dispersed in composite resin⁽⁸⁾ with a resultant higher modulus of elasticity (10.3 GPa). This is consistent with the findings of a previous study⁽²¹⁾ stated that increasing the filler content of composites will increase their elastic modulus.

A possible explanation for the difference in wear (weight loss) may be related to the difference in microstructures, filler content and ceramic or polymer content which may have a detrimental effect on wear behavior and surface roughness of tested CAD-CAM restorative materials⁽²²⁾. Also, the material with a low modulus may be subjected to elastic deformation inducing fatigue than those with a high modulus that may be subjected to abrasion⁽²³⁾. The abrasive wear has worn away the soft polymeric matrix with subsequent plucking out of the exposed filler particles. Additionally, stress concentration at the filler-matrix interface may cause detachment of loose superficial filler, subsurface cracks, and finally loss of the material⁽²⁴⁾. So, initially, the wear may be influenced by the antagonists' surface roughness, but later on, it was affected by the material's intrinsic properties⁽²²⁾. Also, artificial aging in different storage mediums and environmental conditions to simulate the oral environment's destructive capacity is beneficial to better predict material durability and enhance the clinical implications of data⁽²⁵⁾.

The results of this study were in accordance with a previous study⁽²⁶⁾ that explained the wear behavior of the resin composites may be due to the type and size of dispersed fillers. They assumed that resin composites with larger filler size should reveal

higher wear, while those with smaller filler size could be compacted densely exposing less polymer matrix to the wear process and thus assumed to reveal less wear.

SEM micrograph after chewing simulation confirm this suggestion showing a few detached numbers of medium-sized fillers for 3D printed (VS) specimens instead of small and medium-sized filler for milled (BC) specimens as shown in Figures 2 and 3 which are probably responsible for the opposing antagonist enamel abrasion. The chipping of enamel occurs because it is loaded transversally to its prismatic structure which is weaker than when stressed parallel to its prismatic orientation⁽²⁷⁾.

The third null hypothesis tested in this study was partially rejected. No significant difference in Ra value was noticed at baseline between the tested groups but after chewing simulation, the milled (BC) group showed a significant reduction in Ra value, and smoother surfaces were obtained as shown in Table 4, Figure 4. Nevertheless, an insignificant percentage change in Ra value between tested groups ($p=0.74$) was noticed by Chi square test, a higher percentage change of Ra was found in the milled (BC) group (-3.75%). This could be attributed to the bidirectional sliding as scratches from one sliding direction were overrun by the abradant in the opposite direction⁽²⁸⁾.

This recorded Ra value at baseline is comparable to that recorded in a previous study⁽²⁹⁾ following the same polishing protocol. All recorded Ra values were not above 0.2 μm which is critical for bacterial adhesion with subsequent risk of caries and periodontal inflammation. The recorded Ra values recorded in this study were consistent with previously published data (Ra 0.2-3.0 μm)⁽⁸⁾. The polishing action to the opposing enamel antagonist may be attributed to the lower elastic modulus of the indirect resin composite⁽²⁰⁾. SEM images illustrate a similar pattern of angular fillers distribution in the resin composite as shown in Figure 3. Little variations in surface roughness between the tested

groups at baseline highlight efficient polishing protocol followed. No significant difference in Ra value was noticed at baseline and after chewing simulation for the enamel antagonists opposed by tested groups, So the fourth null hypothesis in this study was accepted. Nevertheless, an insignificant percentage change in Ra value between enamel antagonists opposed by tested groups ($p=0.88$) was noticed by Chi square test, a higher percentage change of Ra was found in antagonist opposed with the milled (BC) group (-0.53%).

The correlation between surface roughness and weight loss (wear) of the tested groups was calculated by using Pearson's correlation coefficient which showed an insignificant weak correlation in both the specimens and their opposing enamel antagonists. Accordingly, the fifth null hypothesis was accepted. These results are consistent with that of Ludovichetti et al⁽⁹⁾ who found lack of relation between the two properties, while some studies^(30,31) reported opposite results to findings of the present study.

A higher load of 98 N was applied in this study according to a previous study⁽³²⁾ to simulate the situation in patients with increased chewing forces. The chewing simulation was performed for 60000 cycles to simulate 6 months of clinical performance subjecting the specimens to a mixture of attrition and fatigue wear⁽¹⁶⁾ with incorporation of thermocycling inducing artificial aging to maximize the wear effect⁽³³⁾. The flat surface of the specimens was preferred to allow a balanced stress distribution in the tested CAD-CAM restorative materials⁽¹⁸⁾. Though enamel is considered the gold standard antagonist, but its highly variable form, fluoride content, and amount of aprismatic hydroxyapatite present make its standardization difficult⁽³⁴⁾.

Although, there is similarity in the composition between of 3D printed (VS) and Z250 composite resin in the percentage of inorganic fillers and presence of Bis-EMA organic matrix. The data available about the 3D printed (VS) material still

limited, so future studies still needed to completely clarify its properties. Also, long term in vivo studies are required to confirm the obtained results.

Limitations of the study

pH cycling is required to evaluate their effect on the wear behavior of a newly introduced 3D printed (VS) restorative materials.

CONCLUSIONS

Within the limitations of this study, the followings were concluded:

1. All tested CAD-CAM restorative materials whether 3D printed (VS) or milled (BC) and their opposing enamel antagonists revealed increased wear as demonstrated by weight loss.
2. Chewing simulation had statistically reduced the surface roughness of milled (BC) group.
3. Chewing simulation had similar effect on the surface roughness of enamel antagonists opposed by all tested CAD-CAM restorative materials.
4. The wear demonstrated by weight loss and surface roughness after chewing simulation did not revealed positive correlation within the tested CAM-CAM restorative materials and their opposing enamel antagonists.

REFERENCES

1. Abduo J, Lyons K, Bennamoun M. Trends in Computer-Aided Manufacturing in Prosthodontics: A Review of the Available Streams. *Int J Dent*. 2014;2014:1-16.
2. Naseer MU, Kallaste A, Asad B, Vaimann T, Rassölkin A. A Review on Additive Manufacturing Possibilities for Electrical Machines. *Energies*. 2021;14(7):1940.
3. Kim GT, Go HB, Yu JH, et al. Cytotoxicity, Colour Stability and Dimensional Accuracy of 3D Printing Resin with Three Different Photoinitiators. *Polymers (Basel)*. 2022;14(5):979. Published 2022 Feb 28.
4. Moon W, Kim S, Lim BS, Park YS, Kim RJ, Chung SH. Dimensional Accuracy Evaluation of Temporary Dental Restorations with Different 3D Printing Systems. *Materials (Basel)*. 2021;14(6):1487. Published 2021 Mar 18.
5. Scientific Studies on VarseoSmile Crown plus. Available online: https://www.bego.com/fileadmin/user_downloads/Mediathek/3D-Druck/Scientific-Studies/VarseoSmileCrown-plus/EN/de_81022_0000_br_en.pdf (accessed on 19 May 2021).
6. Eldwakhly E, Ahmed DRM, Soliman M, Abbas MM, Badrawy W. Color and translucency stability of novel restorative CAD/CAM materials. *Dent Med Probl*. 2019;56(4):349-356.
7. Gracis S, Thompson VP, Ferencz JL, Silva NR, Bonfante EA. A new classification system for all-ceramic and ceramic-like restorative materials. *Int J Prosthodont*. 2015; 28(3):227-235.
8. Matzinger M, Hahnel S, Preis V, Rosentritt M. Polishing effects and wear performance of chairside CAD/CAM materials. *Clin Oral Investig*. 2019;23(2):725-737.
9. Ludovichetti FS, Trindade FZ, Werner A, Kleverlaan CJ, Fonseca RG. Wear resistance and abrasiveness of CAD-CAM monolithic materials. *J Prosthet Dent*. 2018; 120(2):318.e1-318.e8.
10. Nguyen JF, Migonney V, Ruse ND, Sadoun M. Resin composite blocks via high-pressure high-temperature polymerization. *Dent Mater*. 2012;28(5):529-534.
11. Zaim B, Serin Kalay T, Purcek G. Friction and wear behavior of chairside CAD-CAM materials against different types of antagonists: An in vitro study. *J Prosthet Dent*. 2022;128(4):803-813.
12. Incesu E, Yanikoglu N. Evaluation of the effect of different polishing systems on the surface roughness of dental ceramics. *J Prosthet Dent*. 2020;124(1):100-109.
13. Barkmeier W, Erickson R, Latta M, Wilwerding T. Wear Rates of Resin Composites. *Oper Dent*. 2013;38(2): 226-33.
14. Myagmar G, Lee JH, Ahn JS, Yeo IL, Yoon HI, Han JS. Wear of 3D printed and CAD/CAM milled interim resin materials after chewing simulation. *J Adv Prosthodont*. 2021;13(3):144-151.
15. Alharbi N, Wismeijer D, Osman RB. Additive Manufacturing Techniques in Prosthodontics: Where Do We Currently Stand? A Critical Review. *Int J Prosthodont*. 2017;30(5):474-484.
16. Nawafleh N, Hatamleh M, Elshiyab S, Mack F. Lithium Disilicate Restorations Fatigue Testing Parameters: A Systematic Review. *J Prosthodont*. 2016;25(2):116-126.

17. Horcas I, Fernández R, Gómez-Rodríguez JM, Colchero J, Gómez-Herrero J, Baro AM. WSM: a software for scanning probe microscopy and a tool for nanotechnology. *Rev Sci Instrum.* 2007;78(1):013705.
18. Turker I, Kursoglu P. Wear evaluation of CAD-CAM dental ceramic materials by chewing simulation. *J Adv Prosthodont.* 2021;13(5):281-291.
19. Grzebieluch W, Kowalewski P, Grygier D, Rutkowska-Gorczyca M, Kozakiewicz M, Jurczyszyn K. Printable and Machinable Dental Restorative Composites for CAD/CAM Application-Comparison of Mechanical Properties, Fractographic, Texture and Fractal Dimension Analysis. *Materials (Basel).* 2021;14(17):4919. Published 2021 Aug 29.
20. Tokunaga J, Ikeda H, Nagamatsu Y, Awano S, Shimizu H. Wear of Polymer-Infiltrated Ceramic Network Materials against Enamel. *Materials (Basel).* 2022;15(7):2435.
21. Ikejima I, Nomoto R, McCabe JF. Shear punch strength and flexural strength of model composites with varying filler volume fraction, particle size and silanation. *Dent Mater.* 2003;19(3):206-211.
22. Mörmann WH, Ender A, Sener B, Stawarczyk B, Mehl A & Attin T. Wear characteristics of current aesthetic dental restorative CAD/CAM materials: two-body wear, gloss retention, roughness and Martens hardness. *J mech behave biomed mater.* 2013; 20: 113-125.
23. Hutchings, I.M. "Tribology: Friction and Wear of Engineering Materials." *Materials & Design* 13, no. 3 (1992): 187.
24. Duarte S, Sartori N, Phark J-H. Ceramic-Reinforced Polymers: CAD/CAM Hybrid Restorative Materials. *Curr Oral Health Rep* 2016;3:198-202.
25. Tornavoi DC, Sato S, Silva LJ, Agnelli JA, & Reis AC: Analysis of surface hardness of artificially aged resin composites. *Mater Res* 2012;15(1):9-14
26. Sumino N, Tsubota K, Takamizawa T, Shiratsuchi K, Miyazaki M, Latta MA. Comparison of the wear and flexural characteristics of flowable resin composites for posterior lesions. *Acta Odontol Scand.* 2013;71(3-4):820-827.
27. Giannini M, Soares CJ, de Carvalho RM. Ultimate tensile strength of tooth structures. *Dent Mater* 2004;20:322-9.
28. Ge S, Wang S, Gitis N, Vinogradov M, Xiao J. Wear behavior and wear debris distribution of UHMWPE against Si₃N₄ ball in bi-directional sliding. *Wear.* 2008;264(7-8):571-8.
29. Siddanna GD, Valcanaia AJ, Fierro PH, Neiva GF, Fasbinder DJ. Surface Evaluation of Resilient CAD/CAM ceramics after Contouring and Polishing. *J Esthet Restor Dent.* 2021;33(5):750-763.
30. Janyavula S, Lawson N, Cakir D, Beck P, Ramp LC, Burgess JO. The wear of polished and glazed zirconia against enamel. *J Prosthet Dent.* 2013;109(1):22-29.
31. Ghazal M, Kern M. The influence of antagonistic surface roughness on the wear of human enamel and nano-filled composite resin artificial teeth. *J Prosthet Dent.* 2009;101(5):342-349.
32. Lutz F, Krejci I, Barbakow F. Chewing pressure vs. wear of composites and opposing enamel cusps. *J Dent Res* 1992;71:1525-9.
33. Sripetchdanond J, Leevailoj C. Wear of human enamel opposing monolithic zirconia, glass ceramic, and composite resin: an in vitro study. *J Prosthet Dent.* 2014;112(5):1141-1150.
34. D'Incau E, Saulue P: Understanding dental wear. *J Dento-facial Anom Ortho* 2012;15(1):104.